Journal of Thermal Analysis and Calorimetry, Vol. 85 (2006) 2, 401–407

EFFECT OF CHAIN LENGTH OF SOME 2D AND 3D ALKANETHIOLS ON GOLD STUDIED BY DSC AND VOLTAMMETRY

S. H. Gyepi-Garbrah[1*], *P. Šimon*[2] *and R. Šilerová*[1]

[1]Department of Chemistry, University of Saskatchewan, 110 Science Place, Saskatoon, SK S7N 5C9, Canada
[2]Department of Physical Chemistry, Slovak University of Technology, 812 37 Bratislava, Slovak Republic

Striking similarities and differences in the behaviour of two-dimensional (2D) self-assembled monolayers (SAMs) on gold and corresponding three-dimensional (3D) SAMs on gold of two alkanethiols of different chain lengths, hexadecanethiol (HDM) and octadecanethiol (ODM) were investigated as a function of temperature. Cyclic Voltammetry (CV) of the 2D SAMs and Differential Scanning Calorimetry (DSC) of the 3D SAMs were used to study previously unexplained behaviour. CV revealed two transition temperatures in both the HDM and ODM 2D systems. In the DSC studies, both a lower and higher temperature transition was observed in the 3D SAMs of HDM but only one temperature transition was observed in the 3D SAMs of ODM. It was deduced that the lower temperature transitions in the gold-alkanoate nanoparticles were related to interaction between the methyl group chain ends. The lower temperature transition was observed in the 3D system of HDM but not that of ODM because the curvature in the 3D system that is absent in the 2D system reduces the interaction between the alkyl chain ends due to a longer chain resulting in an increased distance between the end groups. It was concluded that the lower transition temperature was attributed to the disordering of the alkyl chains starting from the end closest to the terminal groups.

Keywords: *alkanethiol, cyclic voltammetry, DSC, gold, self-assembled monolayer*

Introduction

A number of interactions that operate in two-dimensional (2D) self-assembly (SA) of molecules on planar surfaces may also be present in the three-dimensional (3D) self-assembled monolayers (SAMs) on spherical particles [1]. Alkanethiol-capped gold samples are SAMs on spherical gold particles and also represent 3D analogues of the SAMs on planar surfaces (2D SAM) and these facts have been well documented [2]. Descriptions of the two systems in this study are shown in Fig. 1.

The energetics of the self-organization and the phase behaviour of alkanethiols chemisorbed on planar gold surfaces are difficult to investigate by traditional calorimetry. In order to overcome the limitations to the structural and dynamic studies that can be performed on the 2D SAMs, 3D SAMs may be exploited [2–12]. The 2D character of SAMs when they are chemisorbed on planar gold surfaces limits the experiments by which they can be probed. Gold stabilized with chemisorbed alkanethiols provide a 3D analogue of 2D monolayers that can be investigated by additional conventional (i.e., 3D) method-

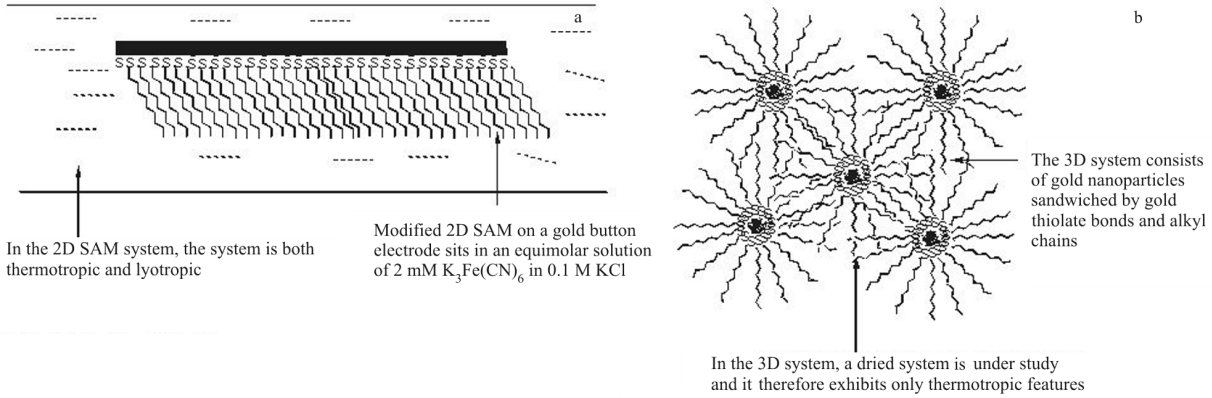

Fig. 1 Description of a – 2D and b – 3D alkanethiol systems

* Author for correspondence: sag577@mail.usask.ca

1388–6150/$20.00

Akadémiai Kiadó, Budapest, Hungary
Springer, Dordrecht, The Netherlands

ologies, including thermal methods like DSC [13]. In DSC [14–19], relatively little sample material is required and the sample can be studied repeatedly on heating and cooling cycles, providing information on reversibility and thermal history effects of phase transformations [16, 20]. It has been reported that these 3D SAMs reveal reversible disordering and ordering of the alkyl chains beginning from the terminal groups and gradually proceeding further down the chain as a function of temperature [13]. Temperature dependent behaviour has also been observed for alkanethiol SAMs on planar gold by electrochemistry [21].

In this work, DSC is used to probe the thermal behaviour of these 3D SAMs and to correlate the results with parallel studies on 2D SAMs using CV in order to investigate previously unexplained behaviour in the SAMs of hexadecanethiol (HDM) and octadecanethiol (ODM) [22]. Structures of HDM and ODM are shown in Fig. 2.

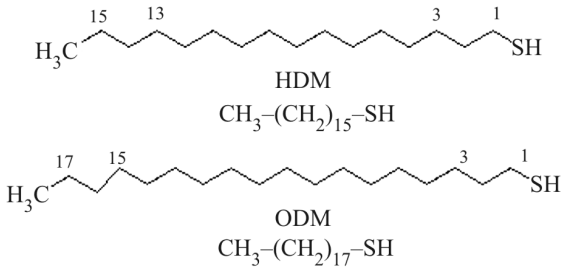

Fig. 2 Alkanethiols used for this study

Experimental

Materials

Chemicals used

HDM (Aldrich, 92%) was redistilled and ODM (Aldrich, 98%) was recrystallized from hexane (BDH). Aqueous solutions were prepared with deionized Millipore water (18.2 M Ω cm^{-1}) obtained from a Milli-Q water system. Bulk polycrystalline gold electrodes (0.0227 cm^2) were obtained from Bioanalytical Systems (BAS). All other chemicals were used as received.

Synthesis of gold-alkanethiol nanoparticles

Gold nanoparticles were derivatized with HDM and ODM to produce alkanethiol-capped gold nanoparticles. The particles ranged in sizes from 2 to 5 nm [23]. They were prepared following the procedure of Brust *et al.* [24]. The reactions were carried out using the ratios of 1.1:1 $HAuCl_4$/alkanethiol. Elemental analysis, Fourier Transform Infra-Red (FTIR), ^1H and ^{13}C NMR spectroscopy were used to characterize the derivatized nanoparticles. DSC was used to study the enthalpy and phase transition of the derivatized nanoparticles.

Methods

Differential scanning calorimetry

The DSC experiments were run using a PerkinElmer DSC-7 with Pyris software. The temperature scale was calibrated using cyclopentane and water (cyclopentane solid/solid temperature –93.43°C, melting temperature of ice 0°C) whilst the enthalpy scale was calibrated to the heat of fusion of ice (6.01 kJ mol^{-1}). The mass of samples used was 3–4 mg. The samples were crimped in standard aluminium pans with an empty pan used as reference. The cooling medium was liquid nitrogen. Helium was used as the purge gas and the heating/cooling rate was 5 K min^{-1}. The sample was first cooled from ambient temperature to –100°C and then heating/cooling cycle in the range –100 to 100°C was reheated three times. At the end of experiment, the sample was examined for any changes in mass.

Electrochemical cell and instrumentation

The electrochemical cell used a conventional three-electrode configuration, with a counter electrode of Pt wire and an Ag/AgCl reference electrode (3M NaCl, BAS). A regular cell was employed for room temperature experiments and a water-jacketed cell connected to a thermostatted water bath (Neslab) was used in the variable temperature measurements. The temperature was monitored directly in the cell by a DP460 Omega thermocouple to ±0.1°C. The whole set-up was enclosed in a grounded Faraday cage. The working electrodes were bulk polycrystalline gold electrodes. CVs were recorded using an EG&G M2783 potentiostat. The data acquisition and control was handled by a computer interfaced to the FRD and potentiostat via an IEEE-488 General Purpose Interface Bus (GPIB) and run with the M270 software for CV. The instruments were calibrated using dummy cells.

Electrode cleaning and monolayer preparation

Bulk polycrystalline gold electrodes were polished on microcloth pads with alumina slurries and rinsed with absolute ethanol and/or water. All gold electrodes previously modified with alkanethiols were cleaned and this has been described in detail elsewhere [22]. The surface roughness of the gold electrodes was determined by under potential deposition (UPD) of copper [25]. After cleaning, the electrodes were im-

mersed in 1–5 mM ethanolic solutions of the alkanethiols and incubated at 23±2°C for times ranging from 24 h to 1 week to form monolayers. Reproducibility of the resulting monolayers (films) was greatly enhanced when the modified electrodes were subsequently incubated for 24 h in Millipore water prior to characterization. The modified electrodes were rinsed with absolute ethanol followed by water prior to CV measurements.

Cyclic voltammetry

After monolayer formation, CV experiments were run in solutions of 3 mM $K_3Fe(CN)_6$ and 3 mM $K_4Fe(CN)_6$ in 0.1 M KCl. Potentials were changed between 0–500 mV at 50 mV s^{-1}. All electrochemical experiments were performed in a Faraday cage. Temperature studies were performed over the range of 10 to 65°C. The temperature was increased with heating rates of 0.5 K min^{-1}. All variations in temperature were initially performed from low to high temperatures (heating), and then from high to low (cooling).

Results and discussion

Variable temperature cyclic voltammetry of modified gold electrodes

The effect of the gold electrode modified HDM and ODM 2D-SAMs on the redox activity of a $[Fe(CN)_6]^{3-/4-}$ probe in solution were studied as a function of temperature. The order of blocking of the redox process $[Fe(CN)_6]^{3-/4-}$ by the modified electrodes is in the order ODM>HDM [22]. The inhibition of the probe by each modified electrode decreased drastically above a certain characteristic temperature, T_{tr} where a large observable redox activity is attained. This increase in observable redox activity above T_{tr} was attributed to an increase in the permeability of the monolayer and drastic increase in current resulting in a phase transition. This phase transition was considered to arise from a change in molecular packing and subsequent melting of chains as the temperature is increased. The drastic change in current can be best observed if a CV of the modified electrode above T_{tr} is superimposed over another one below T_{tr} as shown in Fig. 3 for HDM. CV of bare gold electrode in the same solution is included as reference. This behaviour is also observed for the ODM modified electrode. All the modified electrodes show a different behaviour below and above the characteristic temperature (T_{tr}) specific to each molecular species.

The currents from CVs above T_{tr} from the modified electrodes are close in magnitude to that of the bare gold electrode, and appears that coverage of the

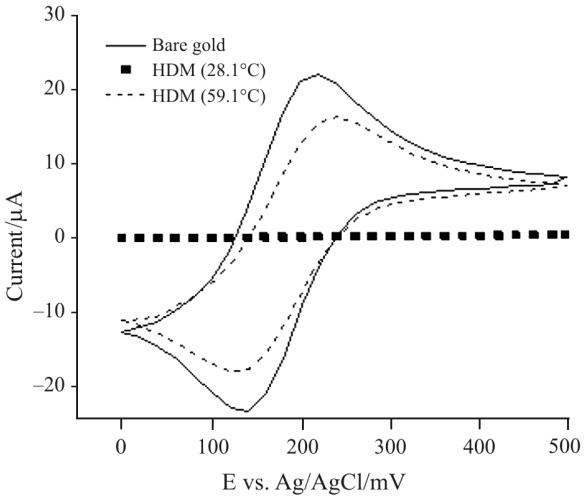

Fig. 3 CV at 50 mV s^{-1} of HDM modified electrodes below and above T_{tr} compared to bare gold in 3 mM $K_3Fe(CN)_6$ and 3 mM $K_4Fe(CN)_6$/0.1 M KCl

modified electrodes are almost zero above T_{tr}. This can be due to non-linear diffusion effects arising from defects and pinholes that expose active sites above T_{tr} and make the CVs appear like that of an array of ultramicroelectrodes [26].

It should be noted that the drastic changes in current observed by CV of the monolayers from the modified electrodes after they have been heated above T_{tr} in solution are not reversible on the time scale of this experiment, generally speaking. Previously heated modified electrodes were re-measured up to two weeks after cooling with no reversibility observed.

Oven studies were also done to find out if the monolayer could be returned to its original state if the resulting process was carried out in air, rather than in solution. A freshly prepared SAM of HDM was heated in an oven from room temperature to approximately 60°C and immediately transferred into a redox probe solution held at 60°C, and a CV taken. The modified electrode was then cooled in the electrochemical cell to 22.0°C. The film of HDM on gold did not recover its original blocking abilities around room temperature as seen in Fig. 4. However, on the comparison with bare gold (also in Fig. 4), it also shows that the HDM-modified electrode heated to 60°C did not reach the response of bare gold around the same temperature.

When the HDM-modified SAM was left in the oven to cool, after heating to 60.5°C, Fig. 5 was obtained. It is worthy of note that this experiment was done in the oven and air, without contact with a condensed fluid phase. However, this type of experiment was not very reproducible. This experimental result most closely follows the solid-state NMR or DSC measurements in which reversibility of temperature-dependent behaviour was observed [15, 20].

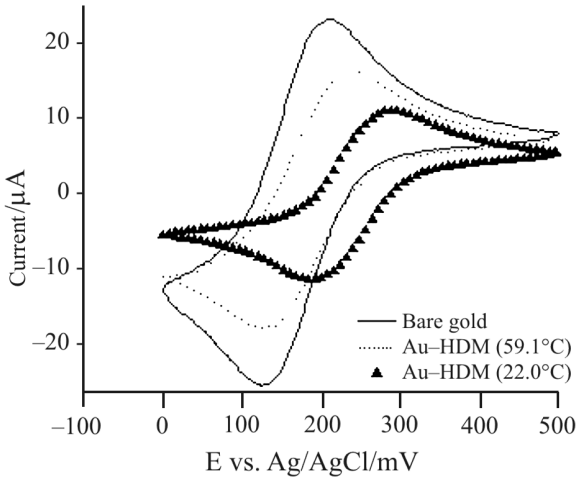

Fig. 4 CV at 50 mV s^{-1} of HDM-modified electrodes heated in an oven and cooled in an electrochemical cell to test for reversibility of monolayer in 3 mM $K_3Fe(CN)_6$ and 3 mM $K_4Fe(CN)_6$/0.1 M KCl

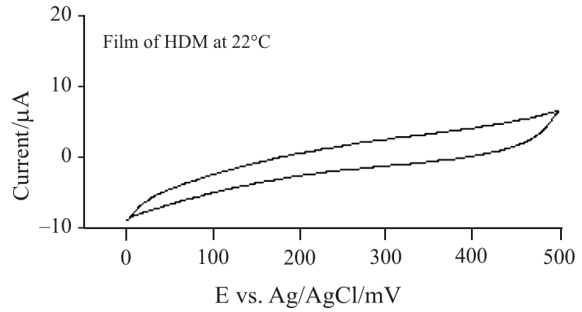

Fig. 5 CV at 50 mV s^{-1} of HDM-modified electrode heated and cooled in air in an oven to test for reversibility of monolayer in 3 mM $K_3Fe(CN)_6$ and 3 mM $K_4Fe(CN)_6$/0.1 M KCl

Cyclic voltammetry – curves from reduction current

The curves for the CV data were plotted as peak reductive current *vs.* temperature. From the curves in Fig. 6, a transition temperature was determined from the CV at where the modified electrode properties change appreciably. The reductive current i_{red} from the redox reaction is plotted as a function of temperature for all modified electrodes and for bare gold, after correcting for overpotential. From the first and second inflexion points in each curve, the T_{tr1} and T_{tr2} may be deduced. Values of T_{tr} extracted from the electrochemical data are listed in Table 1 for modified electrodes of HDM and ODM.

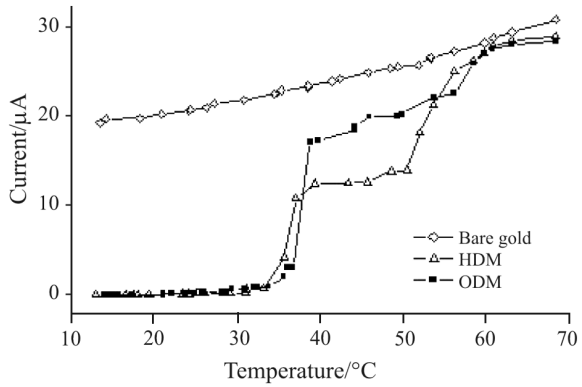

Fig. 6 Temperature dependence of the maximum reductive current from CV of SAMs in 3 mM $K_3Fe(CN)_6$ and 3 mM $K_4Fe(CN)_6$/0.1 M KCl (ν=50 mV s^{-1})

Table 1 Comparison of T_{tr} derived from CV (2D SAMs) and from DSC (3D SAMs)

Method	Species	Transition temp. T_{tr} /°C	
		1st	2nd
CV	HDM	36.8±0.5	42.5±0.5
	ODM	39.2±0.5	48.5±0.5
DSC	HDM	39.9±0.2	48.2±0.2
	ODM	*–	54.5±0.5

*not observed

It should be pointed out that the currents of the modified electrodes above T_{tr} are very high and close to currents of the bare gold electrode. However it should be clearly stated that peak current from CV is not good on its own to explain this phase transition [26, 27]. In the absence of desorption, which has been proved from AC-Electrochemical Impedance Spectroscopy (EIS) data [22, 28], this behaviour can be attributed to non-linear diffusion in the SAMs above T_{tr} where the CV wave resembles that of an array of ultramicroelectrodes arising from defect sites in the SAMs as temperature is increased [29]. Each monolayer has a characteristic temperature at which a distinct discontinuity in the current occurs as observed for SAMs of the same compounds [22].

DSC of derivatized 3D SAMs nanoparticles

DSC was used to characterize the thermal properties of the alkanethiol-capped gold nanoparticles of HDM and ODM. Phase transitions of the nanoparticles are characterized by their temperature and enthalpy [15, 16, 20]. The DSC results confirmed that there was no change of sample mass after the third heating. This indicates that the samples are thermally stable in the temperature region under study. For both samples, the DSC measurements indicate irreversible changes in the structure of the alkanethiol layers during the first and second heating.

Behaviour of HDM-capped gold nanoparticles

The sample gold-HDM exhibited a very small irreversible peak at 39.9°C during the first heating, but in

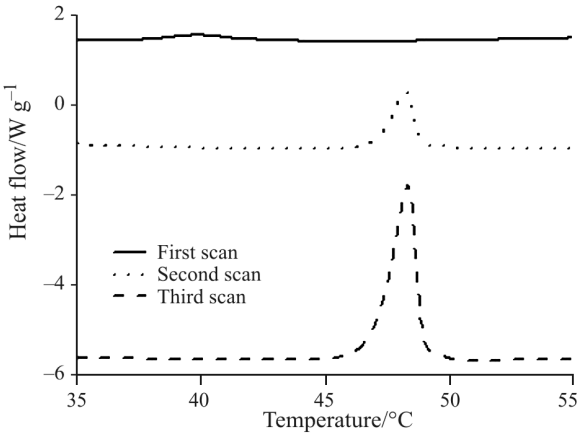

Fig. 7 DSC curves of HDM-Gold

the second heating a sharp quasi-reversible peak corresponding to a phase transition was observed at 48.2°C (Fig. 7). In the third heating the peak (now at 48.4°C) became higher. This behaviour is quite unusual however, it may be attributed to further rearrangements within the nanoparticle. The very small irreversible peak in the first heating (39.9°C) has an ΔH value of the order 1.06 kJ mol^{-1} as indicated in Table 2. This may indicate that, in the freshly prepared sample, there is no tight arrangement of the thiol chains and therefore the small ΔH value could correspond to the rearrangement of the methyl head groups. In addition, there is no indication of a first order phase transition corresponding to the 'melting' of the alkyl chains. However, such a phase transition is observed in the second heating. This suggests that a tight arrangement of the alkyl chain is established only during the first cooling/heating cycle. As seen from the values of ΔH (Table 1) and also from Fig. 7, the peak in the third heating is greater than the peak in the second heating. The onset and peak temperatures of the peaks from the second and third heatings are practically the same. Generally we can say that in the sample gold-HDM, the close-packed arrangement is induced by successive heating/cooling cycles, so that the ΔH of the transition from close-packed to disorder increases over successive cycles. This behaviour is quite similar to that of some metal alkanoates [30].

Behaviour of ODM-capped gold nanoparticles

The sample gold-ODM exhibited quasi-reversible peaks in all heatings. This is shown in Fig. 8. The shape of the peaks and the characteristic temperatures in the first (55.8°C) and second (54.0°C) heating are quite different which suggests a rearrangement of the thiol chains during first heating. In contrast it is seen from the values of ΔH in Table 1 and also from Fig. 8 that the peaks in the second (54.0°C) and third (53.9°C) heating are practically the same implying that there was no rearrangement after the first heating, and thus further heating/cooling cycles are reversible. It is worthy to note that the first irreversible peak observed in gold-HDM was not observed in gold-ODM. This could be explained by the difference in the chain lengths of HDM and ODM, namely the distance of the methyl terminal group from the spherical gold nucleus of the nanoparticles. With an increased distance of the ODM chains from the core metal compared to the shorter HDM chains it is very likely this irreversible peak seen in gold-HDM was difficult to detect in gold-ODM by DSC.

Comparison of thermal behaviour of DSC to that of the electrochemical behaviour from CV

The phase transition temperatures observed by DSC for gold-HDM and gold-ODM is much higher than

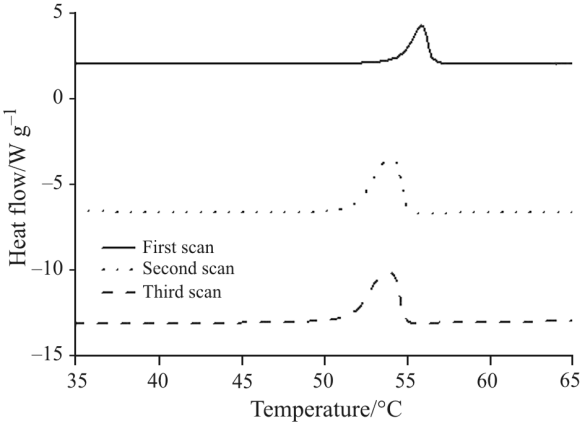

Fig. 8 DSC curves of ODM-Gold

Table 2 Characteristics of peaks from DSC curves

Colloid sample	Heating cycle	Onset temp./°C	Peak max. temp. T_m/°C	ΔH/kJ mol^{-1} of amphiphilic molecule
HDM	1st	37.5	39.9	1.06
	2nd	47.2	48.2	3.84
	3rd	47.0	48.4	13.0
ODM	1st	54.6	55.8	7.93
	2nd	52.0	54.0	6.71
	3rd	51.8	53.9	6.40

those seen by electrochemical methods. However, CV had revealed a set of higher temperature transitions in SAMs of HDM and ODM. These are listed in Table 2.

In the curve of reductive CV current *vs.* temperature (Fig. 6), there is a second high temperature inflexion point that was initially not understood [19]. However, the transition temperatures recorded by DSC corresponded very well with those unexplained high temperature inflexion points observed by CV. If the two inflexion points in the CV data correspond to two different transitions, the question is what then are the two transitions. The DSC detects two transitions in gold-HDM (one irreversible) but only one in gold-ODM (reversible). This could be because the system examined by the DSC experiments is not the same as the SAMs investigated by CV. Specifically, the alkanethiol-capped gold nanoparticles are 3D [13, 24, 27] and spherical while the SAMs are known to be 2D and planar [2]. The cartoon of Fig. 9 illustrates the difference.

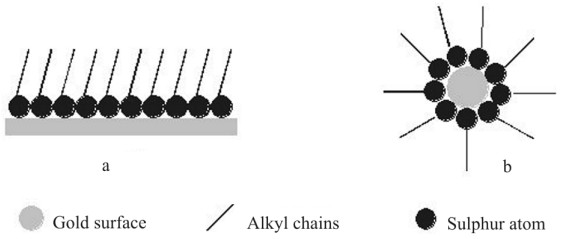

Fig. 9 Cartoon to show the difference between a – planar systems of 2D SAMs of alkanethiols and b – spherical 3D SAMs of alkanethiol-capped gold

If we assume that the lower temperature transition is one that occurs only in the gold-HDM but not gold-ODM for DSC studies, then it could be attributed to head group interactions in 2D planar system. With ODM having a longer alkyl chain length than HDM, the distance from the gold substrate surface to the ends of the alkanethiol head groups is also longer in ODM and thus a corresponding longer distances between individual and adjacent headgroups, because, the longer the chain, the further apart the end groups will be from each other as illustrated by Fig. 9. This makes the head group interaction weaker at the ends. It is therefore not surprising that DSC experiment does not detect the first (irreversible) transition in the ODM system. Furthermore, even though this is detected in gold-HDM, its small energy points more to why in a longer chain like ODM it was non-existent.

The higher temperature transition might then correspond to interchain interactions farther down the chain, which would be present in both planar and in spherical systems. It is reasonable to recognise that the onset of end group mobility occurs at lower transition temperatures and with lower energies, while the onset of chain motion nearer to the gold surface is occurring at higher temperatures and with higher energies.

The T_m of the small irreversible peak during the DSC run for gold-HDM (Fig. 5) agrees well with the lower temperature observed in the HDM modified SAMs. The fact that the small peak observed by DSC was not observed during the next heating/cooling cycle (indicating that it is irreversible), could well explain the lack of success in reversing 2D SAMs to block the redox probe after experiencing the first lower temperature transition [22]. However, it should be noted that the second transition temperature observed by CV for the SAMs of HDM and ODM was not reversible, although that of the nanoparticles was reversible in DSC studies.

Conclusions

CV and DSC have been used to explain the origin of similar phase transitions in 2D and 3D SAMs. This phase transition was attributed to molecular disordering which originates from the terminal region of the chains at lower temperatures and propagates towards the middle of the chain as temperature increases. The detection of the lower temperature depends on the chain length of the alkyl group [31] and the degree of disordering of the chains leading to melting. However, this disorder does not extend to the sulphur head group, an indication that the thiol-gold at the surface of the gold is intact as temperature is increased.

Acknowledgements

One of the authors (P. Šimon) greatly acknowledges the financial support provided within the NATO Science Programme, expert visit grant No. PST.EV.977681.

References

1 M. Sastry, Nanoparticle Thin Films: An Approach Based on Self-Assembly, in: Handbook of Surfaces and Interfaces of Materials, ed. N. Singh, Acad. Press, New York, 2001; Chapter 2, pp. 87–124.
2 A. Badia, R. B. Lennox and L. Reven, Acc. Chem. Res., 33 (2000) 475.
3 W. Gao, L. Dickinson, C. Grozinger, F. G. Morin and L. Reven, Langmuir, 12 (1996) 6429.
4 W. Gao, L. Dickinson, C. Grozinger, F. G. Morin and L. Reven, Langmuir, 13 (1997) 115.
5 M. Kanemaru, Y. Shiraishi, Y. Koga and N. Toshima, J. Therm. Anal. Cal., 81 (2005) 523.
6 L. Reven and L. Dickson, Thin Solid Films, 24 (1998) 149.

7 M. J. Hostetler, J. E. Wingate, C.-J. Zhong, J. E. Harris, R. W. Vachet, M. R. Clark, J. D. Londono, S. J. Green, J. J. Stokes, G. Wignall, G. L. Glish, M. D. Porter, N. D. Evans and R. W. Murray, Langmuir, 14 (1998) 17.
8 D. Li and J. Li, Colloids Surf., A, 257–259 (2005) 255.
9 S. Pawsey, K. Yach, J. Halla and L. Reven, Langmuir, 16 (2000) 3294.
10 G. W. H. Hohne, Thermochim. Acta, 332 (1999) 11.
11 N. Sandhyarani and T. Pradeep, J. Mater. Chem., 10 (2000) 981.
12 N. K. Chaki and K. P. Vijayamohanan, J. Phys. Chem. B, 109 (2005) 2552.
13 A. Badia, W. Gao, S. Singh, L. Demers, L. Cuccia and L. Reven, Langmuir, 12 (1996) 1262.
14 R.Voicu, A. Badia, R. B. Lennox and T. H. Ellis, Chem. Mater., 12 (2000) 2646.
15 R. H. Terrill, T. A. Postlethwaite, C. Chen, C-D. Poon, A. Terzis, A. Chen, J. E. Hutchison, M. R. Clark, G. Wignall, J. D. Londono, R. Superfine, M. Falvo, C. S. Jonson Jr., E. T. Samulski and R. W. Murray, J. Am. Chem. Soc., 117 (1995) 12537.
16 A. Badia, S. Singh, L. Demers, L. Cuccia, G. R. Brown and R. B. Lennox, Chem. Eur. J., 2 (1996) 359.
17 R. Voicu, A. Badia, F. Morin, R. B. Lennox and T. H. Ellis, Chem. Mater., 13 (2001) 2266.
18 S. Strella and P. F. Erhardt, J. Appl. Polym. Sci., 13 (1969) 1373.
19 C. E. Giacomelli and W. Norde, J. Colloid. Interface Sci., 233 (2001) 234.
20 A. Badia, L. Cuccia, L. Demers, F. Morin and R. B. Lennox, J. Am. Chem. Soc., 119 (1997) 2682.
21 A. Badia, R. Back and R. B. Lennox, Angew. Chem. Int. Ed. Engl., 106 (1994) 2332.
22 S. H. Gyepi-Garbrah and R. Šilerová, Phys. Chem. Chem. Phys., 3 (2001) 2117.
24 M. Brust, M. Walker, D. Bethell, D. J. Schiffrin and R. Whyman, J. Chem. Soc. Chem. Commun., (1994) 801.
25 M. R. Deakin and O. Melroy, J. Electroanal. Chem., 239 (1988) 321.
26 C. Amotore, J. M. Saveant and D. Tessier, J. Electroanal. Chem., 147 (1983) 39.
27 A. C. Templeton, W. P. Wuelfing and R. W. Murray, Acc. Chem. Res., 33 (2000) 27.
28 S. H. Gyepi-Garbrah and R. Šilerová, Phys. Chem. Chem. Phys., 4 (2002) 3436.
29 A. J. Bard and L. R. Faulkner, Electrochemical Methods, John Wiley and Sons, Inc., New York, 1980.
30 J. A. R. Cheda, M. V. Garcia Perez, M. I. Redondo Yelamos and A. Sanchez Arenas, J. Therm. Anal. Cal., 76 (2004) 7.
31 J. Lalot, I. Stasik, G. Demailly, D. Beaupère and P. Godé, J. Therm. Anal. Cal., 74 (2003) 77.

Received: January 31, 2005
Accepted: May 22, 2006

DOI: 10.1007/s10973-005-6928-9